EVIDENCE FOR *sap1* AS A VIRULENCE FACTOR IN *Burkholderia cepacia* COMPLEX

A THESIS SUBMITTED TO THE GRADUATE DIVISON OF THE UNIVERSITY OF HAWAIʻI AT MĀNOA IN PARTIAL FULFILMENT OF THE REQUIRMENTS FOR THE DEGREE OF

MASTER OF SCIENCE

IN

MICROBIOLOGY

AUGUST 2017

By

Andrew P. Bluhm

Thesis Committee:

Tung T. Hoang, Chairperson
Stuart P. Donachie
Sladjana Prišić

Dedication

This work is dedicated

to the bridge builders of the past;

the shoulders of those we stand on

in an effort to see one iota more

over the horizon.

Acknowledgements

I would like to thank Dr. Tung Hoang for taking a chance on me and extending an invitation to become a part of his lab. The opportunity to conduct research at a level that many do not get to experience has been instrumental in shaping me as a person. Thank you for your years of support and guidance, and I wish you much luck and all the funding in the future.

I would also like to thank my committee members Dr. Stuart Donachie and Dr. Sladjana Prišić for their time, input, and expertise during my time here. The future of the department and its graduate students are better off thanks to your investment of time and care. I'd also like to thank Dr. Maqsudul Alam for his time, insight and enthusiasm.

A significant portion of this research was done while surrounded by a fantastic group of young researchers, both former and current. Dr. Yun Kang, Dr. Michael Norris, Jan Zarzychi-Siek, Zhenxin Amy Sun, Ian McMillan, Darlene Cabanas, Hung Vo and Dawson Fogen – from rigorous scientific discussions to comedic relief, I am truly thankful I shared our home away from home with you.

I would also like to thank my parents for their naïve wonder at what I was doing in the lab, and the unfathomable amount of love and support they have shown me throughout my life.

Abstract

Burkholderia cepacia complex (Bcc) is a consortium of at least 20 closely related Gram negative species that are a risk factor for cystic fibrosis (CF) patients. Previously in *B. pseudomaelli*, a hypothetical protein with no known function, was identified to be a novel virulence factor and involved in attachment. In this work, highly conserved homologs in Bcc K56-2 and LO6 were examined in multiple *in vitro* and *in vivo* models such as attachment to eukaryotic cell lines, biofilm attachment and formation, *Caenorhabditis elegans* survival model, *Drosophila melanogaster* feeding model, and mouse lung infection. We found that the deletion mutants had impaired attachment and biofilm formation, and significantly lower *in vivo* survival and replication, compared to the wildtype strains. Finally, *C. elegans* and mice infected with the mutants had better survival compared to wildtype infections, supporting the hypothesis that the protein surface attachment protein 1, or *sap1*, is a virulence factor.

Table of Contents

List of Tables

List of Figures

List of Abbreviations

AHL	acylated homoserine lactone
Ap	ampicillin
Ap^r	ampicillin resistant/resistance
Bcc	*Burkholderia cepacia* complex
BLAST	basic local alignment search tool
Bp	*Burkholderia pseudomaelli*
BSA	bovine serum albumin
$CaCl_2$	calcium chloride
Ce	*Caenorhabditis elegans*
CF	cystic fibrosis
CFTR	cystic fibrosis transmembrane conductance regulator
CI	competitive index
CIP	calf intestinal alkaline phosphatase
Cm	chloramphenicol
Cm^r	chloramphenicol resistant/resistance
cPhe	chlorinated phenylalanine
DAP	diaminopimelic acid
Dm	*Drosophila melanogaster*
DMEM	Dulbecco's Modified Eagle Medium
DMSO	dimethyl sulfoxide
Ec	*Escherichia coli*

eDNA	extracellular deoxyribonucleic acid
EDTA	ethylendiamionotetraacetic acid
EPS	exopolysaccharide
FBS	fetal bovine serum
FRT	Flp recognition target
g	gram
g	gravitational force
GC	guanine-cytosine
gat	glyphosate acetyltransferase
Gm	gentamicin
Gm^r	gentamicin resistant/resistance
GS	glyphosate
k	kilo
kb	kilobase pair
kDa	kilodalton
Km	kanamycin
Km^r	kanamycin resistant/resistance
LB	Luria-Bertani
Mbs	mega base pairs
MG	minimal glucose
mg	milligram
$MgSO_4$	magnesium sulfate
mL	milliliter

mM	millimolar
ng	nanogram
NGM	nematode growth media
nmol	nanomole
OD	optical density
*ori*T	origin of transfer for conjugation
PBS	phosphate buffered saline
PCR	polymerase chain reaction
pheS	gene encoding a mutated **α**-subunit of phenylalanyl tRNA synthase
pmol	picomoles
QS	quorum sensing
rRNA	ribosomal ribonucleic acid
sap	surface attachment protein
SDS	sodium dodecyl sulfate
SEM	standard error of the mean
spp	species
Tel	tellurite
Tel^r	tellurite resistant/resistance
TLR5	Toll-like receptor 5
TNFR1	tumor necrosis factor receptor 1
Tp	trimethoprim
Tp^r	trimethoprim resistant/resistance
U	Units of activity

v/v	percent volume/volume aqueous concentration
w/v	percent weight/volume dissolved concentration
µg	micrograms
µL	microliters
µM	micromolar

Chapter 1: Introduction

1.1 *Burkholderia cepacia* Complex

Burkholderia cepacia complex (Bcc) is a consortium of at least 20 closely related Gram negative, non-spore forming bacilli species (1). Species within Bcc have up 78% of their genes in common, with genomes ranging from 7 to more than 9 Mbs that are typically divided amongst 3 chromosomes and a plasmid (2). They have an average GC content of 67%, and possess numerous gene duplications, insertion sequences, and mobile elements (3, 4). This plasticity is thought to contribute to their ability utilize a variety of metabolic pathways and thus improve their resiliency (5, 6). Another benefit is the increased mutation rate of the genome when stressed, such as in infections (7). Bcc gets its namesake from the 1950 characterization of *B. cepacia* as a pathogen of onions by W.H. Burkholder, who identified it at the time as *Pseudomonas cepacia* (8). Further isolates continued to be classified under the genus *Pseudomonas* until 1992 when they were transferred to the genus *Burkholderia* based on molecular factors including 16S rRNA sequencing, DNA-DNA hybridization values, fatty acid composition and phenotypic characteristics (9). This redesignation also suggested that *B. cepacia* was a single type strain, which lasted five years until it was demonstrated using *recA* gene sequencing that there were at least five distinct species, or genomovars, comprising *B. cepacia* (10). The proposed and accepted solution was to umbrella those genomovars under the new coined *Burkholderia cepacia* complex. Today there are ten recognized genomovars (I-X) which have been given their own speciation, as well as further speciation and subtyping based on advances in whole genome sequencing, global transcriptional analysis and past methods such as

ribotyping, multilocus enzyme electrophoresis, and pulse field gel electrophoresis (Table 1) (1, 5).

While originally identified as a pathogen of plants, Bcc gained notoriety especially for infecting immunocompromised individuals and cystic fibrosis (CF) patients. The first reports occurred in the 1970s and 1980s, with one coining the "cepacia syndrome" when describing patients at a Toronto CF center, being categorized by necrotizing pneumonia, bacteremia, and sepsis, along with high levels of morbidity and mortality (12, 13). Sequencing and molecular epidemiological studies of the more virulent Bcc species led to understanding that the pathogen can be passed from person, leading to implementation of strict segregation guidelines (14, 15). Additionally, treatment with antibiotics was ineffective due to innate antibiotic and antimicrobial resistance (16, 17). These epidemic strains are the focal point of understanding the virulence of this highly problematic opportunistic human pathogen group.

1.2 Cystic Fibrosis

Having an autosomal recessive disorder, CF patients are born with mutations within the cystic fibrosis transmembrane conductance regulator (CFTR) gene which encodes a protein responsible for chloride and bicarbonate transport in epithelial cells found in multiple organ systems (18, 19). It affects mostly those of Caucasian/European decent at a rate of 1 in 1000 births and has over 2000 gene variants divided into six main classes (19). The most predominant mutation known as Phe508del or ΔF508 and prevents CFTR from properly incorporating into epithelial cell membranes (19, 20). This is the most common mutation accounting for 66% of CF cases worldwide and 90% of CF cases in the USA (19–21). This deletion leads to impaired

mucociliary clearance, increased amounts of mucus, and changes the pH of airway surface liquid in the lung (20, 22). All of these symptoms foster an excellent environment for pathogens, making the lung infection the main cause of CF patient mortality (20, 23–25). Major constituents of CF infections are opportunistic pathogens such as *Haemophilus influenzae*, *Staphylococcus aureus*, and *Pseudomonas aeruginosa* (18, 26). Most of these pathogens' virulence can be effectively limited by periodic treatment that reduces the bacterial load in the lung (18, 25, 26). However, upon acquisition of Bcc, lung function continues to decline despite treatment (18). Even total lung transplants, currently the closest approximation to a "cure", cannot secure survival, often leading to Bcc-positive patients to be excluded from transplant lists (28, 29). These cases of reinfection are still not totally understood, but it is thought that the ability to survive intracellularly and disseminate among different organs contributes to that outcome (30–32). For patients infected with Bcc, 20% will suffer from cepacia syndrome, leading rapidly to patient death and if not, Bcc will become a chronic infection by adapting to the lung environment for as long as the patient lives (33, 34). Due to the reduced opportunity and effectiveness of treatment for Bcc infections, CF patients depend on a better understanding of how Bcc is able to create and maintain disease.

1.3 Virulence Factors Used for Attachment by Bcc

The diversity and resilience of Bcc leads to the current understanding that there are overlapping layers of virulence factors that contribute to disease, especially in regards to attachment – a prerequisite for invasion of eukaryotic cells (31, 35, 36). Understanding the mechanisms behind these traits is key to developing treatment for both chronic and acute disease

(37). Some are identified as notable factors including cable pili, flagella, autotransporters, outer membrane proteins, lipoproteins, exopolysaccharide (EPS) biosynthesis and biofilm formation (11, 38–44).

Cable pili are long multimer structures that have been shown to allow for bacterial interaction and grouping (45). Additionally, when associated with a 22-kDa adhesin, Bcc utilize cytokeratin 13 as a receptor to bind to eukaryotic cells in the CF lung (45, 46). Outside of motility, flagella are another means of Bcc attachment and invasion of host cells (30). Interestingly, studies show that after infection is underway, Bcc can suppress flagella expression if transitioning to a chronic infection or if isolated from the blood (33, 47). This finding makes sense, as Bcc flagella can be recognized by Toll-like receptor 5 (TLR5) and triggers an inflammatory signaling cascade in the host's immune response, possibly preventing the dissemination (48).

Autotransporters are proteins of the type V secretion system that are able to incorporate themselves into the bacterial membrane to secrete or act as an effector on the extracellular milieu (49). Recently, the Bcc autotransporter BcaA was found to bind to tumor necrosis factor receptor 1 (TNFR1) on lung epithelial cells, as well as provide protection from serum mediated death (41, 50).

EPS production is an important part of Bcc species' ability to maintain a chronic infection (51). EPS are various long branching polysaccharides that are secreted into the extracellular milieu and can confer protection from host mediated defenses while also promoting attachment and persistence (52, 53). One of the more common Bcc EPS is cepacian, which is linked to protection from clearance in the lungs as well as a component of the thicker Bcc biofilms (51, 53). Biofilms are complex bacterial communities that produce EPS and extracellular DNA (eDNA), which protect from host defenses and increase resistance to antibiotics in the CF lung

(54, 55). The ability for Bcc to form biofilms is independent of genomovar classification, but instead are linked to production of acyl-homoserine lactones (AHLs) and other quorum sensing molecules (56). Interestingly, Bcc is often a co-inhabitant of *Pseudomonas aeruginosa* biofilms in the CF lung, which leads to a "cross-talk" from *P. aeruginosa* quorum sensing signals and contribute to the biofilm even if the Bcc strain forms weak biofilms by itself (57, 58). For some Bcc species, the biofilm maintains close proximity of the bacteria and epithelial cell junctions, aiding in Bcc to squeeze through the junctions via paracytosis (59).

Other genes in Bcc may be involved in attachment and biofilm formation and hypothetical proteins found within the genomes should be characterized. Previously, we identified in *Burkholderia pseudomallei* (*Bp*) a hypothetical protein involved in attachment and localized to the surface of the bacteria. Furthermore, the mutant strain was completely attenuated after 60 days in an intranasal mouse infection model (manuscript in preparation). This protein has a highly conserved homolog in many Bcc species (two examples of Bcc type strains shown in Figure 1), prompting the hypothesis that this protein is a virulence factor for Bcc as well (60).

1.4 Research Aims

The goal of this work was to test the hypothesis that the hypothetical protein surface attachment protein 1 or *sap1* (XM57_RS04855 in *B. cepacia* LO6 and BURCENK562V_RS004960 in *B. cenocepacia* K56-2) is a virulence factor involved in attachment. This was accomplished by deletion mutant construction and complementation, followed by utilization of *in vitro* and *in vivo* models to determine the extent of involvement of *sap1* in attachment and pathogenesis.

Chapter 2. Materials and Methods

2.1 Bacterial Strains, Cell Culture and Growth Conditions

All strains used and generated, as well as plasmids in this study are listed in Table 2 and 3. Bcc and *E. coli* were cultured using Luria-Bertani (LB) medium (Difco) or 1× M9 minimal medium supplemented with 20 mM glucose, 500 μM $MgSO_4$, and 25 μM $CaCl_2$ (MG), and following additives when appropriate: trimethoprim (100 μg/mL for *E. coli*, 200 μg/mL for K56-2, 300 μg/mL for LO6), tetracycline (10 μg/mL for *E. coli*, 50 μg/mL for K56-2, 150 μg/mL for LO6), tellurite (10 μg/mL for *E. coli*, 125 μg/mL for Bcc) chloramphenicol (20 μg/mL for *E. coli,* 150 μg/mL for Bcc), glyphosate (0.1% v/v for *E. coli*, 0.4% v/v for Bcc), chlorinated phenylalanine (cPhe, 0.1% w/v), and diaminopimelic acid (100 μg/mL).

Derivatives of *E. coli* strain EPMax10B (BioRad), E1345 and E1869 were routinely used for cloning or plasmid mobilization into Bcc as described previously (61, 62).

Human lung epithelial cell line A549 and murine macrophage cell line RAW264.7 were cultured in DMEM containing 4.5 g/L glucose with 4.0 mM L-glutamine (HyClone). All cultures were supplemented with 10% (v/v) heat-inactivated standard fetal bovine serum (FBS; HyClone) and antibiotic/antimycotic solution (100 U/mL penicillin, 100 μg/mL streptomycin, and 250 ng/mL amphotericin B; HyClone). Cells were maintained at 37°C and 5% CO_2 in a humidified incubator. Cell lines were maintained at 50-80% confluence at which point RAW264.7 macrophages were passaged by scraping the cells from the flasks using a cell scraper. A549 cells were passaged by first washing with warmed PBS, followed by a 15 min detachment incubation with 0.25% trypsin-EDTA (Gibson) at 37°C and 5% CO_2 in a humidified incubator. The media-cell suspension was collected, gently pelleted, washed twice with pre-

warmed DMEM, and distributed to new flasks. Cell lines were maintained in Corning™ flasks and plates with CellBIND™ surfaces. Cell concentrations were determined using the Scepter handheld automated cell counter (Millipore).

2.2 General Molecular Techniques

2.2.1 Oligonucleotides

Oligonucleotides were synthesized through Integrated DNA Technology and are listed in Table 4. All molecular methods and their components utilized were employed as previously described (61).

2.2.2 Reagents

All restriction enzymes, DNA markers, T4 DNA polymerase, T4 DNA ligase, calf intestinal alkaline phosphatase (CIP), deoxynucleoside triphosphates (dNTPs) were purchased from New England Biolabs (NEB) and used as recommended by the supplier. *Pfu* and *Taq* DNA polymerases were purchased from Stratagene.

2.2.3 Polymerase Chain Reaction (PCR)

PCR was generally performed by initial denaturation at 94^{o}C for 3 min and 30 cycles of 15 s at 94^{o}C, 15 s at 50 – 70^{o}C (determined by the melting temperature of primers), and 1 min per kb at 72^{o}C, with a final step of 10 min extension at 72^{o}C. Fifteen pmol to 30 pmol of forward and reverse primers, 10 ng – 100 ng DNA template and 5 U of *Pfu* DNA polymerase were used per 50 μL reaction. Dimethyl sulfoxide (DMSO) at 2.5 – 10% (v/v) was supplemented to the PCR reactions when some of the GC rich chromosomal regions of Bcc chromosome were difficult to

amplify. Additional steps taken to assist with difficult amplification, *Taq* polymerase was mixed with *Pfu* at a 1:5 ratio when the downstream application of the PCR product was not sensitive to the adenine that *Taq* can add to the end of the PCR product.

2.2.4 Gel Electrophoresis and DNA Extraction

Various DNA samples can be separated based on their size difference on 1-2% agarose gel by running at 110V for 60 min. SYBR® Safe stain was used for the visualization of the DNA fragments. DNA bands of desired sizes were excised from agarose gel and DNA was extracted by using Zymo Gel Recovery Kit (Zymo Research Corporation) following the manufacturer's protocol.

2.2.5 Isolation of Bacterial Chromosomal DNA and Plasmid DNA

Three mL of overnight culture was used to isolate *E. coli* and Bcc chromosomal DNA utilizing the phenol-chloroform extraction protocol (63).

Zyppy Plasmid Miniprep I kit (Zymo Research Corporation) was used for isolation of plasmid DNA from *E. coli* grown overnight by following the supplier's instruction.

DNA concentrations were measured using a Thermo Scientific NanoDrop^{TM} 1000 Spectrophotometer according to the manufacturer's protocol.

2.2.6 Restriction Enzyme Digestion and Ligation

Restriction enzyme digestions were usually incubated at 37^{o}C for at least 2h. To de-phosphorylate vectors, CIP was added directly to the digestion mixture followed by 30 min incubation at 37^{o}C. If necessary, gel electrophoresis was used to purify the restriction enzyme

digestion mixture to allow subsequent enzyme digests.

A 10:1 molar ratio of insert DNA fragments to vector DNA was used for ligation. Generally, a final volume of 10 μL was used for a ligation reaction with 1 U T4 DNA ligase in 1x ligation buffer. The ligation reaction was incubated at 16^{o}C for at least 4 h. Ligation mixtures were routinely transformed into various *E. coli* strains according to the need.

Electro-competent *E. coli* cells were prepared as described previously, and chemically competent *E. coli* cells were prepared via the $MgCl_2/CaCl_2$ method as described previously (63, 64).

2.3 General Techniques

2.3.1 Bacterial Conjugation

E. coli mobilizable strains E1354 and E2072 were routinely used as donor strains to introduce vectors containing *ori*T into Bcc recipient strains. Helper plasmid pRK2013 was used as an alternative to mobilize plasmids into *E. coli* and Bcc. Briefly, the donor and recipient strains were grown up to mid-log phase in LB broth, at which point 0.5 mL of each culture was gently mixed in a sterile 1.5 mL microfuge tube and spun down at 7,000× *g*. The cell pellet was gently resuspended in 20 μL of LB broth and spotted on a pre-warmed LB agar plate. After overnight growth, the cells were scraped off and washed with 1 mL of 1x M9 salt buffer twice, and dilutions were plated on the appropriate selective media.

2.3.2 Construction of Mutants and Complementation Strains

Bcc strains K56-2 and LO6 were mutated utilizing pKaKa-OOT-*comE-crp* for both strains (65). Briefly, pKaKa-OOT-*comE-crp* was tri-parentally conjugated into each Bcc strain assisted

by pRK2013 and selected on MG and appropriate tetracycline concentration. For mutant construction, pFRT-Tp-*pheS* was used as PCR template with primers O3093-3096. After gel electrophoresis and purification, 5µl containing 1 µg of the ~2.2 kb PCR product was co-incubated with pelleted mid-late log Bcc strains containing pKaka-OOT-*comE-crp* at room temperature for 30 minutes. The co-incubation mixture was recovered in 4 mL of LB for 4 hours shaking at 225 RPM after which the culture was harvested and plated on LB + Tp200 (K56-2) or LB +Tp300 (LO6). Resulting colonies were purified on their respective media, and screened for proper deletion via PCR. Once confirmed, the strains were grown in LB to mid-log and saved in glycerol at -80°C. Verified mutants were then tagged using the mini-Tn7-*gat-rfp* plasmid as described (66). Successful transposition was verified with PCR of the four *glmS* sites and fluorescent microscopy.

Complementation also utilized the mini-Tn7 based integration method (61, 66). Briefly, Bcc genomic DNA was used as template for PCR with respective primers (O3297-O3300) to amplify the *sap1* gene, as well as introducing KpnI digestion sites on either side to be cloned into mini-Tn7-*gat-gfp* linearized by KpnI. The resulting plasmids, mini-Tn7-*gat-gfp-sap1*_K56 and mini-Tn7-*gat-gfp-sap1*_LO6, were then digested with PstI and XhoI to replace the *gat* gene with a similarly digested pwFRT-P_{CS12}-Tel^r, in order to differentiate strains in competition assays. Additionally, a Cm^r cassette was cloned in by BspHI and BglII digestion of pPS854-*FRT*-Cm^r and the appropriate complementation vector. Restriction digest verified the plasmids' size and orientations. Genomic integration of the complementation vectors mini-Tn7-Cm-tel-*gfp-sap1*_K56 and mini-Tn7-Cm-tel-*gfp-sap1*_LO6 was done as previously described and verified by PCR and florescent microscopy (66).

2.4 Growth Characterization of Mutants and Complementation Strains

Wildtype, mutant, and complemented strains were grown to stationary phase, subcultured 1:200 into 250 mL of LB in a 500 mL flask and grown at 37°C and 225 RPM. Aliquots of 250 µL were pulled at designated times, added to 750 µL ddH_20 in cuvettes, and absorbance was read via spectrophotometer at 630 nm.

2.5 Attachment Assays

The attachment assay was carried out by dilution of bacterial strains in PBS and plated on LB. Colonies were counted to determine the number of CFU used to initiate the infection and calculate attachment efficiencies. The dilutions were used to infect the cell cultures in 24-well CellBIND plates at an MOI of 10:1. After 30 minutes, the bacteria-containing medium was removed and the monolayers were washed 3 times with pre-warmed PBS. Monolayers were lysed with 0.2% Triton-X100 in PBS, diluted, plated onto LB and incubated at 37°C for 48 h. Colonies were enumerated and attachment efficiency was determined by dividing the attached number by the initial number of bacteria. The experiment was carried out in triplicate and the numbers represent the average of all three replicates with the error bars representing the SEM. The unpaired student *t*-test was used to determine the significance of attachment efficiencies between the wildtype, mutants, and complements.

2.6 Biofilm Crystal Violet Assay

Quantification of biofilm production was tested as previously described with modifications (67, 68). Briefly, bacterial strains were grown to late log, subcultured at 1:200, and 125 µL

dispensed into Costar Serocluster™ 96-well microtiter plates (Corning) with each strain being replicated ten times. Uninoculated media served as a negative control. The outside perimeter of the 96-well plates was filled with ddH_2O to minimize evaporation from wells. After 18 hours (the time of maximum biofilm production based on unpublished observations), wells were rinsed with ddH_2O and patted dry. At this point, half of the wells were filled with 150 µL of 1% (w/v) crystal violet for 15 minutes, rinsed, and let air dry. The other wells were filled with 150 µL of 0.1% (w/v) SDS resuspension mixture and mixed via repeated pipetting and scraping of the sides. The resulting resuspensions were then serially diluted and plated on LB to enumerate CFUs. The crystal violet stained wells were solubilized with 200 µL of a modified biofilm dissolving solution of 80% ethanol + 10% SDS (w/v), with 150 µL transferred to a flat-bottomed 96-well microtiter plate and read for absorbance at 550 nm (69). The student *t*-test was used to determine the significance of differences in biomass and CFUs between the wildtype, mutants, and complements.

2.7 *Caenorhabditis elegans* Survival Studies

Each bacterial strain was plated on three plates with nematode growth media (NGM) and allowed to grow as lawns for 36 hours; fifteen L4 age-synchronized *Caenorhabditis elegans* (*Ce*) were added to each plate for a total of 45 worms for each Bcc strain (70, 71). *E. coli* OP50 was used as a food source as well as a negative control. Worms were observed daily and deaths were recorded. The experiment was conducted twice with comparable results.

2.8 *Drosophila melanogaster in vivo* Competition Study

Flies studies were preformed as described previously with modifications (72). Briefly, wildtype Oregon R flies were maintained on standard cornmeal sucrose medium. Bacterial strains were washed in a 5% sucrose + PBS solution, and adjusted to a final 1:1 ratio totaling ~2.5×10^{10} CFU/mL, of which 150 µL was added to Whatman filters atop 5 mL of 5% sucrose agar in vials and allowed to dry at room temperature for 30 minutes. Twelve 1-3 day old male flies were starved for 3 hours and added to each vial, with three vials for a total of 36 flies used per Bcc strain combination. As a control, the mixtures were also plated on 5% sucrose agar without flies to monitor the ratio over time. At two and four days post-inoculation, three flies from each vial were taken for CFU enumeration, with each vial's flies being treated separately. Serial dilutions of the fly homogenate were plated onto LB (CFU_{total}) or LB with chloramphenicol and tellurite ($CFU_{complement}$). CFU_{mutant} was determined from the difference of CFU_{total} and $CFU_{complement}$ the ratio of which to yields the *in vivo* CI ($CFU_{mutant}/CFU_{complement}$).

2.9 Imaging of the *D. melanogaster* Crop

Additional flies from the above CI experiments were sacrificed; the crops and gastrointestinal tract (GI) were carefully removed under a dissection microscope and cured in ProLong Gold Antifade reagent (Invitrogen). A cover slip was placed over the organs and pressed flat to remove air bubbles, and sealed with clear nail polish applied along the edges. After letting cure while covered for 30 minutes, the slides were imaged using a Zeiss Observer D1 with AxioCam MRc5 and accompanying Axiovision 4.9.1 software.

2.10 Animal Studies

Frozen aliquots of the strains were plated to determine accurate CFUs. Bacteria used for inoculations were washed in PBS, diluted to the desired concentration, and plated at the start of the study to accurately determine the number of CFUs used. Six-week-old female BALB/c mice were purchased from Jackson Laboratories. Before challenge, the mice were anesthetized by intraperitoneal injection of 100 mg/kg ketamine and 10 mg/kg xylazine. For the CI studies, 40 µl of the 1:1 mutant/complement (~7×10^7 CFU/mouse) strain mixture was inoculated intratracheally using the BioLITE Intubation System (Braintree Scientific), with PBS used as a control. Five mice were used per group. The same 1:1 mixture was also plated for comparative CFU changes as a further control. After 3 or 5 days, mice were humanely euthanized after which their lungs were harvested and homogenized in 5 mL PBS. Serial dilutions of the homogenate were plated onto LB (CFU_{total}) or LB with chloramphenicol and tellurite ($CFU_{complement}$). CFU_{mutant} was determined from the difference of CFU_{total} and $CFU_{complement}$ the ratio of which to yields the *in vivo CI* ($CFU_{mutant}/CFU_{complement}$) (73).

For survival studies, mice were similarly inoculated intratracheally with ~3×10^8 CFU/mouse with five mice used per strain. After 10 days, surviving mice were humanely sacrificed and their lungs, livers, and spleens were homogenized in 5 mL PBS for serial dilution and CFU enumeration.

Chapter 3: Characteristics of *in vitro* and *in vivo* Virulence Assays

3.1 Introduction

Bcc as an opportunistic pathogen is troubling due to the morbidity and mortality rate associated with the infection in CF patients, due to the lack of effective treatments (3, 74). One of the strategies in dealing with Bcc is sequestration of CF patients from one another, in an effort to curb the nosocomial aspect of Bcc infection and is not actually a treatment for patients infected with Bcc (1). Furthermore, Bcc maintains a multitude of virulence factors, as well as an ability to mutate the genome when present with a stressful environment only increases resiliency (4, 5). Additionally, the CF environment itself does not lend to easy access to the bacteria for removal or killing via host factors and antibiotics (24, 75). To compound the issue, Bcc is able to vacate the extracellular milieu and invade host epithelial cells, as well as prevent degradation within host phagocytes (30, 35, 76). Some of the genes involved in these processes lie within a significant Bcc genomic profile, hypothetical proteins, and provide an opportunity to understand some of the unique quirks of this pathogenic group (2, 47, 77, 78).

The *Bp sap1* homolog has been shown to be involved in attachment and virulence while sharing high homology and identity with Bcc *sap1,* which lends high confidence that some properties will also be conserved as a virulence factor (Figure 1A). However, due to the hypothetical nature of the protein, a suite of assays were used to identify multiple aspects of potential virulence. Here, we examined the Bcc hypothetical protein *sap1* to determine the extent of its involvement in attachment.

3.2 Results

3.2.1 K56-2 and LO6 Share Similar *sap1* Homology and Genomic Organization

The strains K56-2 and LO6 were used due to having sequenced genomes, as well as success using the mutagenesis protocols. Additionally they represent multiple genomovars and distinct lineages; the K56-2 strain related to an epidemic isolate ET-12 that coursed through CF wards in Canada, the United Kingdom, and Europe (38, 79). LO6 is a clinical isolate from Thailand that was recently sequenced and is similar to another Bcc species, *B. dolosa* (60, 80, 81). At the chromosomal level, 5kb upstream and downstream of their respective *sap1* homologs shares 90% identity within 84% of that region in question (Figure 1B).

3.2.2 Bacterial attachment to eukaryotic cells involves *sap1*.

To determine if the Bcc *sap1* homolog was involved in attachment, mutants were constructed using the lambda-red recombineering system (65) and complemented using the mini-Tn7 based integration system (61, 66). To ensure that any observed differences between the strains were only due to the absence or presence of a functional *sap1* gene, the strains' growth kinetics were observed. The strains showed no significant difference in the growth rates between the mutants, complements, and wildtype (Figure 2). These strains were used in attachment assays in two different eukaryotic cells lines: A549 human lung epithelial cells and RAW264.7 murine macrophages (Figure 3). Of all combinations, K56-2 strains saw the highest attachment to A549 cells, yet the mutant displayed an 8-fold decrease in attachment ($p=0.0165$) (Figure 3A). That mutant also experienced nearly a 5-fold decrease in attachment to murine macrophages ($p=0.028$) (Figure 3B). For LO6 strains, the mutant exhibited a 3-fold attachment deficiency in A549 cultures ($p=0.0026$) (Figure 3C), while over a 60-fold decrease in attachment to

RAW264.7 cells (p=0.0106) (Figure 3D), the largest defect overall. Wildtype strains showed no significant difference from the complemented strains for either species. These data suggest that *sap1* is involved in attachment for Bcc strains K56-2 and LO6, and that the chromosomally located complement restores the defect of the mutants seen in this model.

3.2.3 *sap1* Effects Biofilm Formation *in vitro*

Biofilm formation is a virulence factor especially for CF lung infections due to up-regulation of biofilm related genes (56) as well as the transition of clinical CF isolates to a mucoid phenotype over time (82). Given the involvement of *sap1* in attaching to eukaryotic cells, we also sought to assay if the attachment was utilized for attachment to solid surfaces and biofilm formation *in vitro* and as it pertains to virulence in the well-established *Ce* model (38, 83, 84). Bacterial strains were grown to late log, subcultured and dispensed into 96-well plates for the crystal violet biomass assay (Figure 4A, 4D), and determination of CFUs within the biomass attached to the wells' walls (Figure 4B, 4E). Generally, LO6 wildtype and complement strains produced nearly a 10-fold increase in biomass when compared to respective K56-2 strains, yet the LO6 *sap1* mutant displayed nearly the same level of biomass as its K56-2 counterpart (Figure 4A, 4D). Interestingly, the CFUs recovered from the K56-2 *sap1* mutant had nearly an 8-fold decrease (p=0.1741), considering there was only about a 20% decrease in biofilm biomass (p=0.0007) (Figure 4A, 4B). The LO6 *sap1* mutant, while producing a much more robust biofilm, lost over 46-fold CFUs and had a 10-fold loss in biofilm biomass ($p<0.0001$; p=0.0103) (Figure 4D, 4E). These decreases in the LO6 *sap1* mutant point to *sap1* playing a significant complementary role in LO6 biofilm formation.

3.2.4 Virulence of Biofilm Production is Influenced by *sap1*

To determine the virulent effects of biofilm formation with and without *sap1*, strains were assayed by determining the survival rate of *Ce* when allowed to graze on the respective bacteria. The experiment was conducted twice with similar results (data for one experiment shown, n=45). The K56-2 wildtype and complemented strains saw longer survival than their LO6 counterparts; the LO6 strains had a markedly shorter survival curve with total death occurring in nearly half the time (Figure 4C, 4F). Both mutant strains had similar survival curves, with total death occurring near the 200-hour mark. When comparing the biofilm *in vitro* data to the *Ce* survival curves, the *Ce* worms grazing on poor biofilm producers experienced longer survival, and the strains with strong biofilm formation led to shorter *Ce* survival curves.

3.2.5 *D. melanogaster* Model Shows a Decrease in Mutant Competitiveness *in vivo*

The strains were also used in the fruit fly feeding model, which has been shown to be useful in determining *in vivo* bacterial fitness, a surrogate model for internal *in vivo* biofilm formation, and a means to corroborate the *Ce* data in another well-established invertebrate model (72, 85, 86). At two and four days post-inoculation, flies were taken to enumerate bacterial loads while additional flies were used for fluorescent imaging of the crop. CFU enumeration of each strain allowed for determination of the Competitive Index (CI), a metric to compare the fitness of the mutant against the complement, as a ratio of their respective CFUs. When CI < 1, the mutant is less competitive than its complement strain when grown together in that environment; the smaller the number, the less competitive the mutant strain. While the CI of the inoculum control did not show a change over time, the CI of K56-2 stains showed that the complement was able to significantly outcompete the mutant three-fold at day 2 ($p=0.0007$), and maintained that advantage to day 4 ($p=0.0008$) (Figure 5A). LO6 strains had a similar result, with a three-fold

advantage at day 2 ($p=0.0007$), and nearly doubling that advantage on day 4 ($p<0.0001$) (Figure 5B). Overall, the mutants showed a marked disadvantage in their ability to compete with the complement when adapting to the environment within the fly. Representative fluorescent images corroborate this, with hardly any RFP-tagged mutants being visible. The autofluorescence of the crop can be seen in the background, with the tagged bacteria seen as points of fluorescence scattered throughout the crop.

3.2.6 Mouse Model of Bcc Infection Shows a Decreased Fitness and Lethality of the *sap1* Mutant

The importance of *sap1* was further investigated in the more complex mouse lung. BALB/c mice were inoculated via intratracheal intubation to assay the CI of mutant and complement, as well as monitor survival at higher doses of wildtype, mutant and complement. Based on pilot studies to determine the proper infectious dose and time window of infection, K56-2 was not able to colonize the BALB/c lungs, leading to LO6 exclusively being used for this animal study. After inoculation with an equal ratio of mutant to complement totaling $\sim 7\times10^7$ CFU/mouse, the CI at 3 dpi showed a significant 5-fold decrease in the fitness of the mutant ($p<0.0001$), and continuing to decrease to nearly a 10-fold difference at 5 dpi ($p<0.0001$) (Figure 6A). At day 3, the bacterial load of complements recovered was above the inoculum, which indicated that the complement was able to replicate and outcompete the mutant when colonizing the lung environment.

Survival studies were also conducted with an inoculum of $\sim 3\times10^8$ CFU/mouse. The mice inoculated with the *sap1* mutant (n=4) experienced 75% survival at 10 dpi, compared to 20% and 40% of the wildtype (n=5) and complement (n=5), respectively (Figure 6B). Lungs, livers, and

spleens of the surviving mice were harvested to determine bacterial loads (Figure 7). Interestingly, all organs were infected except for the liver from one Δ*sap1*-infected mouse, which had no detectable bacteria (Figure 7B). The lungs from the wildtype and complement infected mice retained a bacterial load that was above or comparable to the inoculum. This indicates LO6 was able to replicate and persist in the lung, while also disseminating to other organs, while the *sap1* mutant exhibited significant defects in ability to colonize and disseminate

Chapter 4: Discussion

In this work, we provide evidence of the hypothetical Bcc protein *sap1* as a virulence factor based on its involvement in attachment and pathogenesis. Characterization of *sap1* up to this point was lacking: a hypothetical protein containing only domains of unknown function that has limited homology outside the genus. Based on the fact that there are multiple ways for Bcc to present virulence, a variety of assays were utilized. Since the *sap1* homolog in *Bp* shared a high identity and was identified to be involved in attachment, the first step was to determine if the Bcc *sap1* could attach to eukaryotic cells.

LO6 wildtype and *sap1* complement exhibited similar attachment efficiencies in both epithelial and phagocytic cell lines. This finding was comparable to the K56-2 wildtype and complement strains' attachment ability to RAW264.7. In contrast, both mutant strains experienced decreased attachment efficiency to the epithelial and macrophages eukaryotic cells. Looking at the defect of the mutant strains' ability to attach, there was not a consistently better cell type for attachment: LO6 saw the largest defect on RAW264.7 cells while the K56-2 mutant's largest defect was attaching to A549s. This observation does not provide evidence for a specific target of Sap1 protein to either A549 or RAW264.7 cells, but does show an involvement in the attachment process. The fact that Bcc attaches to human and mouse cell lines underscores the importance of elucidating the role *sap1* plays in pathogenesis.

While K56-2 strains exhibited nearly double the attachment efficiency in the A549 cells, K56-2 displayed a lower pathogenicity in the *Ce* kill curves compared to LO6. K56-2 was also unable to replicate and colonize the mouse lung. As for the biofilm assay, the low K56-2 biofilm production is not entirely unexpected, as our lab's previous work has used LO6 in biofilms studies specifically over K56-2 due to its higher ability in forming biofilm in the drip flow

model. This robustness was not uniform, as the LO6 mutant could only produce biomass similar to all three K56-2 strains and CFUs recovered – the K56-2 mutant did not exhibit a significant difference in bacterial load within the biofilm compared to the wildtype ($p=0.1741$). Surprisingly, the LO6 wildtype and complements were able to harbor nearly 46-fold more bacteria in roughly 10-fold the biomass. This high cell density could have an effect on the amount of quorum sensing molecules present and the factors they regulate, or any contact dependent virulence factors (19, 20, 27). Taken together, these factors may contribute to the LO6 strains' increased morbidity in the nematode model and maintain an infection in the BALB/c model.

Compared to K56-2, LO6 did not have the same deficiencies in maintaining an infection in the mouse model, as the lungs of the surviving mice contained a bacterial load at or slightly higher than the inoculum of wildtype and the complement. In this study there are no other factors potentially masking an attachment defect in the *sap1* mutant, since there was no use of agar beads, mucoid strains, or co-infections with other pathogens. These are often used to mimic various forms of chronic infections which was outside the objective of these studies (11, 57). In this work, the *sap1* mutant was still able to maintain a presence in the lung after 10 days, pointing to other virulence factors contributing to infection. Due to the opportunistic nature of Bcc, it is probable that the virulence factors establishing infection are an amalgamation of factors to exploit the weakness of the host, and may require a shift in environment to express those factors, such as changes from the upper to lower respiratory track (87, 88). Considering that the Bcc genome is known to increase in mutation rate when under stress, it would be interesting to see a comparative analysis of the recovered bacteria from the lungs, liver and spleen and compare it to the inoculum (4, 47, 89).

Overall, the data herein strengthens the hypothesis that *sap1* is involved in attachment and can be described as a virulence factor. Its role in pathogenesis can be hypothesized to be one of many tools Bcc uses to entrench in the CF lung by interacting with the sputum found in the CF lung, or adhesion to the lung epithelial cells. The close proximity to the already damaged lung epithelial cells might then draw the attention of various host immune system cells. If those host cells do recognized the pathogen, Bcc could be phagocytized and therefore protected from the innate immune system, while being shuttled to the spleen, liver and/or lymph nodes. To better understand this interplay, future research should focus on targeting the ligand *sap1* interacts with, resolving the protein's structure, and determining if it is immunoprotective for treatment and potential vaccine development.

Tables

Table 1 Bcc genomovars and first descriptors

Species	Genomovar	Reference
B. cepacia	I	(10)
B. multivorans	II	(10)
B. cenocepacia	III	(10, 90)
B. stabilis	IV	(91)
B. vietnamiensis	V	(10)
B. dolsa	VI	(80)
B. ambifaria	VII	(92)
B. anthina	VIII	(93)
B. pyrrocinia	IX	(93)
B. ubonensis	X	(81)
B. latens	–	(94)
B. diffusa	–	(94)
B. arboris	–	(94)
B. seminalis	–	(94)
B. metallica	–	(94)
B. contaminans	–	(95)
B. lata	–	(95)
B. pseudomultivorans	–	(96)
B. stagnalis	–	(97)
B. territorii	–	(97)

Table 2. Bacterial strains used in this study

Strain	Lab ID	Genotype/Description	Reference or source
Bcc			
B. cepacia LO6	P754	Prototroph; cystic fibrosis isolate	P. Sokol
LO6 Δ*sap1*	E3691	Δ*sap1*:: FRT-Tp^r-*pheS/att*Tn7::miniTn7-*gat-rfp*	This work
LO6 Δ*sap1*/comp	E3695	Δ*sap1*:: FRT-Tp^r-*pheS/att*Tn7::miniTn7-Cm-tel-*gfp-sap1*_LO6	This work
B. cenocepacia K56-2	E1554	Prototroph; cystic fibrosis isolate	P. Sokol
K56-2 Δ*sap1*	E3237	Δ*sap1*:: FRT-Tp^r-*pheS*/ *att*Tn7::miniTn7-*gat-rfp*	This work
K56-2 Δ*sap1*/comp	E3693	Δ*sap1*:: FRT-Tp^r-*pheS/att*Tn7::miniTn7-Cm-tel-*gfp-sap1*_K56	This work
E. coli			
DH5α	E0272	*F− φ80dlacZΔM15 Δ(lacZYA-argF)U169 endA1 recA1 hsdR17(rK − mK +) supE44 thi-1 ΔgyrA96 relA1*	Lab collection
EPMax10B-*pir116* Δ*asd* Δ*trp*::Gm^r *mob*-Kan^r	E1354	Kan^r, Gm^r, F$^-$ λ$^-$ *mcrA* Δ(*mrr-hsdRMS-mcrBC*) φ80d*lacZ* Δ*M15* Δ*lacX74 deoR recA1 endA1 araD139* Δ(*ara, leu*)7697 *galU galKrpsL nupG* Tn-*pir116-FRT2* Δ*asd::wFRT* Δ*trp*::Gm^r-*FRT5 mob*[*recA*::*RP4-2* Tc::Mu-Kan^r]	Available lab strain
EPMax10B-*lacI*^{q} pir	E1869	F$^-$ λ$^-$ *mcrA* Δ(*mrr-hsdRMS-mcrBC*) φ80d*lacZ* Δ*M15* Δ*lacX74 deoR recA1 endA1 araD139* Δ(*ara, leu*)7697 *galU galKrpsL nupG lacI*^{q}*-FRT8 pir-FRT4*	Available lab strain
EPMax10B-Δ*dapA*::Gm^r-*lacI*^{q}-*pir leu+ mob*-Kan^r	E2072	F$^-$ λ$^-$ *mcrA* Δ(*mrr-hsdRMS-mcrBC*) φ80d*lacZ* Δ*M15* Δ*lacX74 deoR recA1 endA1 galU galKrpsL nupG* Δ*dapA*:: *lacI*^{q}*-FRT8 pir*-Gm^r *leu+ mob*[*recA*::*RP4-2* Tc::Mu-Kan^r]	Available lab strain

Table 3. Plasmids used in this study.

Plasmids	**Lab ID**	**Relevant properties**	**Reference**
pRK2013	E0272	Kan^r, helper plasmid encoding conjugative proteins	(98)
pPS854-*FRT*-Cm^r	E0855	Ap^r; Cm^r; plasmid with Cm^r-*FRT*-cassette	
pwFRT-P_{CS12}-Tel^r	E1584	Tel^r;P_{CS12}-Tel^r cassette flanked by wildtype *FRT* sequences	(64)
mini-Tn7-*gat-gfp*	E2462	GS^r, mini-Tn7-gat harboring *gfp*	(62)
mini-Tn7-*gat-rfp*	E2326	GS^r, mini-Tn7-gat harboring *rfp*	(62)
mini-Tn7-Cm-tel-*gfp-sap1*_K56	E3697	Cm^r; Tel^r; mini-Tn7 harboring *gfp* and K56 *sap1*	This work
mini-Tn7-Cm-tel-*gfp-sap1*_LO6	E3699	Cm^r; Tel^r; mini-Tn7 harboring *gfp* and LO6 *sap1*	This work
pTNS3-asd_{Ec}	E2237	Suicidal helper plasmid containing *E. coli asd* and transposase for the Tn7 site-specific transposition system	(61)
pKaka-OOT-*comE-crp*	E3217	Tet^r; broad-host-range λ-red helper plasmid based on Tet resistance that also confers DNA uptake	In preparation
pFRT-Tp^r-*pheS*	E2964	Tp^r, Ap^r, *FRT1* flanked Tp^r-*pheS* cassette	(64)

Table 4. Primers used in this study

Primer number and name	Sequence
876; TN7L	5'-ATTAGCTTACGACGCTACACCC-3'
3093; V_C0817 pheS-gat dw	5'-GATCCACAGCGCAACGGCCCGGCATGCGCCGGGCCGTGATCGGTTCAGCTGGCACGACAG-3'
3094; V_C0817 pheS-gat up	5'-AAACACATAGCTAACCCAGCCTGGTGCCCGCAAGCCTGGAGACAGGGCGATTAAGTTGGG-3'
3095; V_C0817 pheS-M13 dw END	5'-TGCGCGATCCACAGC-3'
3096; V_C0817 pheS-gat up END	5'-TCACCTTTAAACACATAGCTAAC-3'
3097; V_C0817 pheS-gat dw screen	5'-GCATTCGGTTCGGTCGG-3'
3098; V_C0817 pheS-gat up screen	5'-TGTGCTTGCTATCGTTTACCG-3'
3099; glmS1 Bc K56-2	5’-GTGTGAAACCACTTCGTCTTG-3’
3100; glmS2 Bc K56-2	5’-GAAGATCGTGCTCGGCGAAATG-3’
3101; glmS3 Bc K56-2	5’-TTCCTGCGTTCGGTGCCAGTCG-3’
3102; glmS4 Bc K56-2	5’-CCGAGCTGCTGAAGAACACC-3’
3166; BamHI V_C0817 miniTn7	5'-TATATGGATCCGCGGGAATGGACG-3'
3167; PstI V_C0817 miniTn7	5'-ATATCTGCAGTGGAATCGTTTCGGATG-3'
3169; L06 PstI V_C0817 miniTn7	5'-ATATCTGCAGCGATAAATTCATATCGTTTCGGC-3'
3170; L06 BamHI V_C0817 miniTn7	5'-TATATGGATCCGCGCGTTACTGCTTGAT-3'
3214; HindIII V_C0817 mT7gRFP	5'-ATATAAGCTTGGAATCGTTTCGGATG-3'
3215; SpeI V_C0817 mT7gRFP	5'-TATATACTAGTCGCGGGAATGGACG-3'
3216; LO6 HindIII V_C0817 mT7gRFP	5'-ATATAAGCTTCGATAAATTCATATCGTTTCGGC-3'
3217; LO6 SpeI V_C0817 mT7gRFP	5'-TATATACTAGTCGCGCGTTACTGCTTGAT-3'
3297; KpnI V_C0817 dn	5'-TATATGGTACCGCGGGAATGGACG-3'
3298; KpnI V_C0817 up	5'-ATATGGTACCTGGAATCGTTTCGGATG-3'
3299; L06 KpnI V_C0817 dn	5'-TATATGGTACCGCGCGTTACTGCTTG-3'
3300; L06 KpnI V_C0817 up	5'-ATATGGTACCGATAAATTCATATCGTTTCGGC-3'
3499; LO6 glmS1	5'-GGTACCGACGTCGACAAGC-3'
3500; LO6 glmS2	5'-CGACAAGCCGAGGAATCTGG-3'
3501; LO6 glmS3	5'-GCTGCTCGCGTATCACACC-3'

Figures

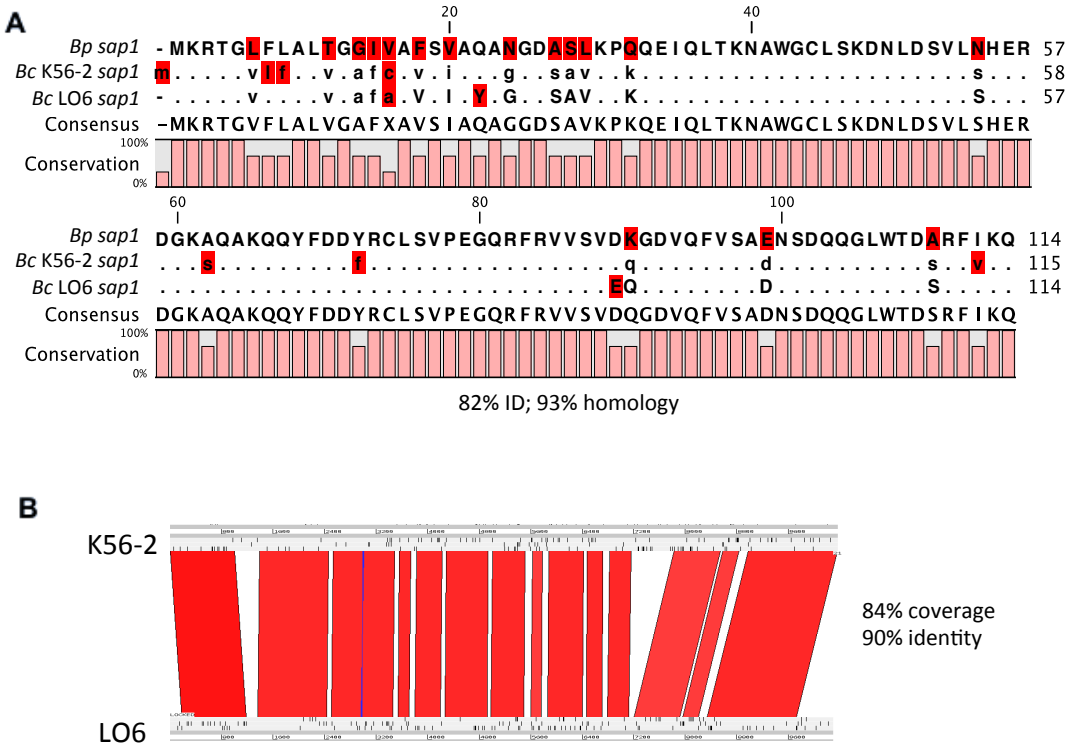

Figure 1. Alignment of *sap1* amino acid sequence and surrounding DNA sequence. (A) Alignment of *sap1* from *Bp* K96243, *B. cenocepacia* K56-2 and *B. cepacia* LO6 using CLC Sequence Viewer 7. – denotes a gap; . denotes conservation; mismatches are highlighted in red. (B) Syntany map of 5 kb up- and down-stream of the K56-2 and LO6 *sap1* using Artemis webACT. Identical regions are indicated in red, non-identical regions in white, and blue indicates a region that is inverted in the two strains.

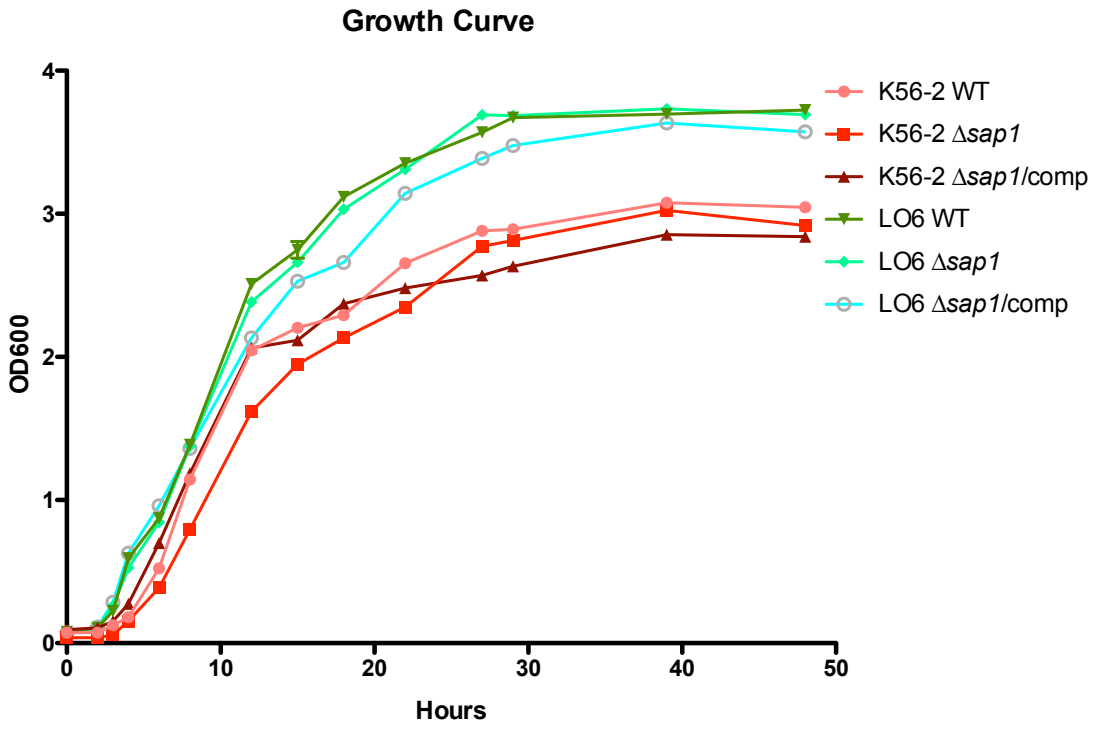

Figure 2. Growth curves of Bcc K56-2 and LO6 strains. No significant differences were observed among the various K56-2 strains or LO6 strains over 48 hours.

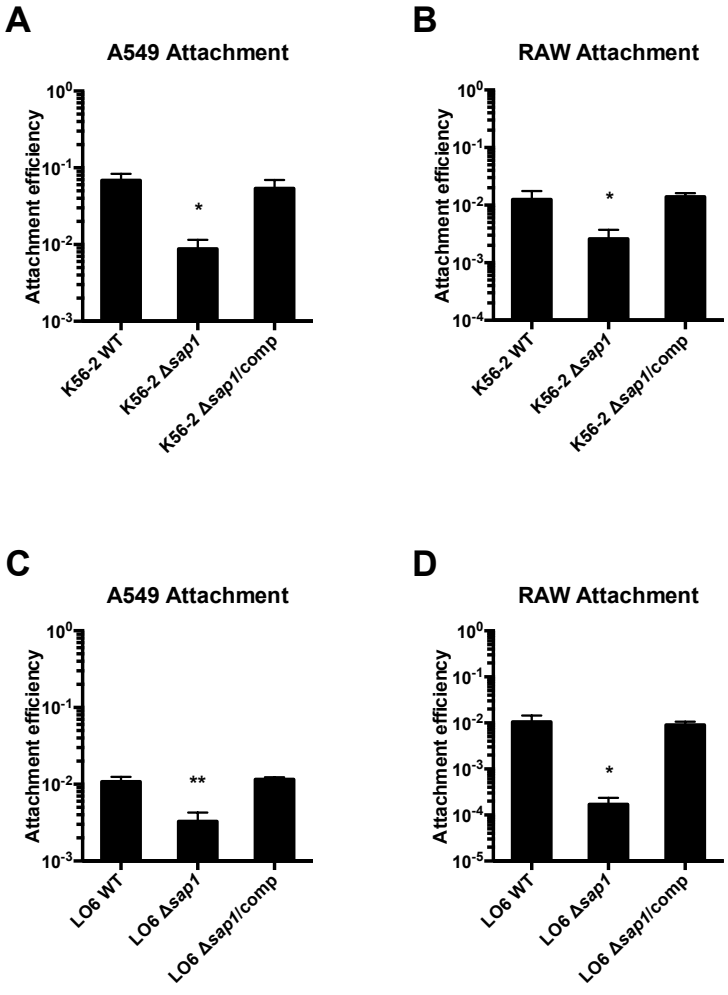

Figure 3. *sap1* involved in attachment to eukaryotic cells. Wildtype, mutant, and complemented strains' CFU recovered divided by the inoculum amount from attachment assays done in triplicate: (A and B) *Bc* K56-2 and (C and D) *Bc* LO6 exposed to A549 human epithelial cells and RAW264.7 mouse macrophages. Error bars signify SEM; * $p<0.05$, ** $p<0.005$, as determined by unpaired student *t*-test. Wildtype=WT.

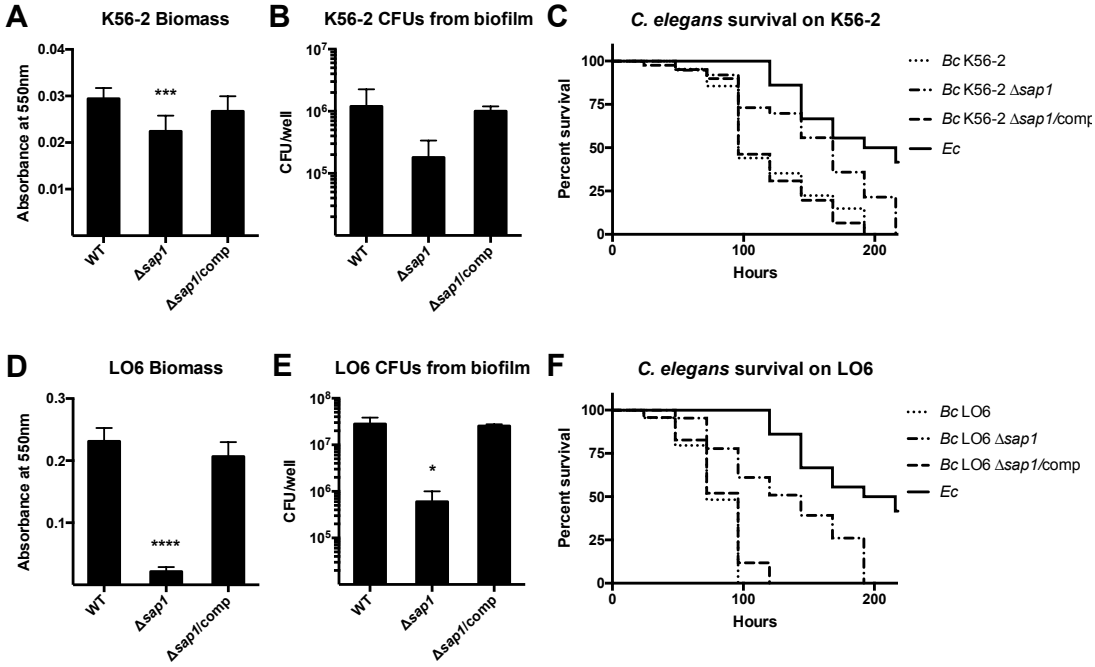

Figure 4. Biofilm production and *C. elegans* survival is influenced by *sap1*. Biofilm production and CFUs within the biofilm for (A, B) K56-2 strains or (D, E) LO6 strains. Error bars signify SEM; * $p<0.05$, ** $p<0.005$, *** $p<0.0005$, **** $p<0.0001$, as determined by unpaired *t*-test. Effects of (C) K56-2 strains or (F) LO6 on *C. elegans* grazing on the wildtype, *sap1* mutant, complement, or *Ec* strains; 45 worms per strain were used. Wildtype=WT.

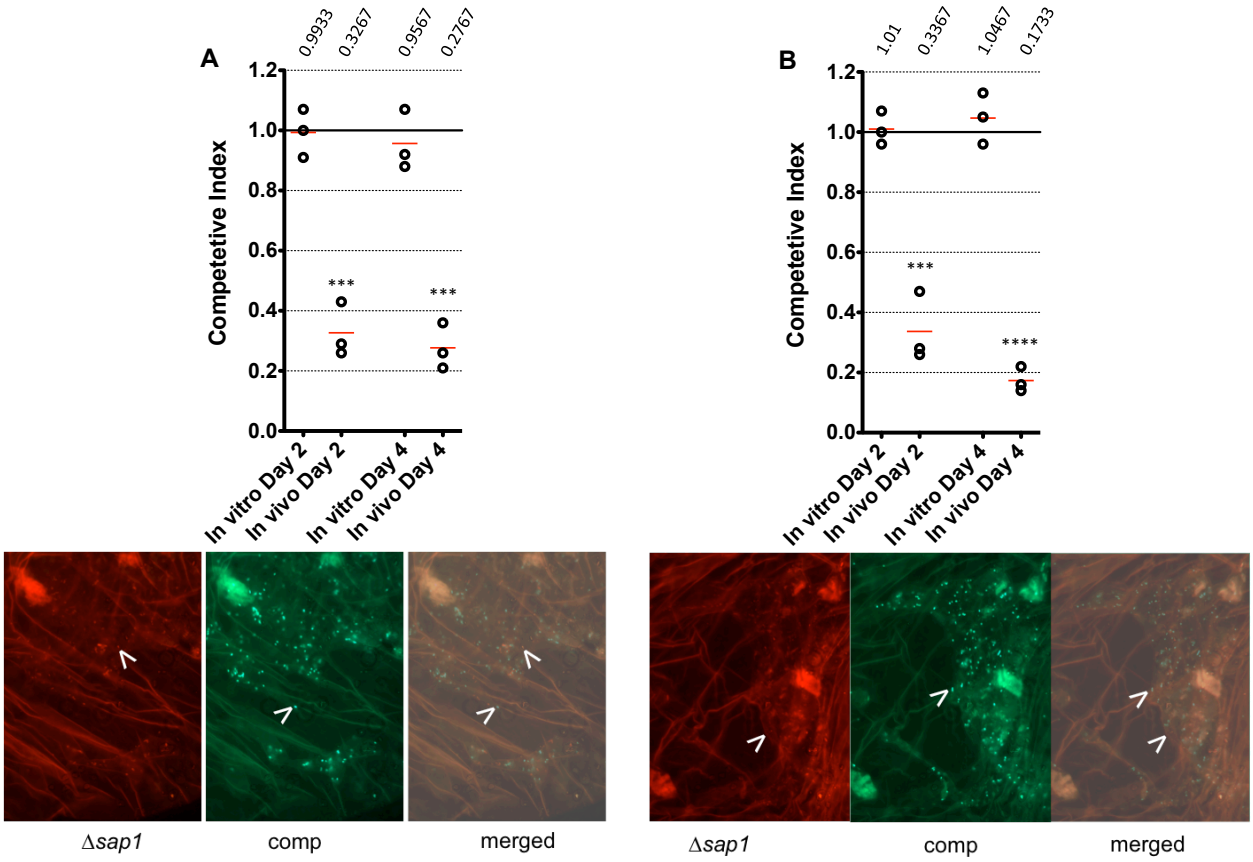

Figure 5. Comparative fitness in the *D. melanogaster* feeding model. CI of (A) K56-2 or (B) LO6 strains after 2 or 4 days of either exposure to grazing flies or *in vitro* control with no flies. Each dot is the CI of a set of 3 flies from one vial, with the geometric mean of the triplicate listed above. Representative images from each strain as Δ*sap1* (RFP), complement (GFP) and merged channels are listed below; carots indicate bacteria. *** $p<0.0005$, **** $p<0.0001$.

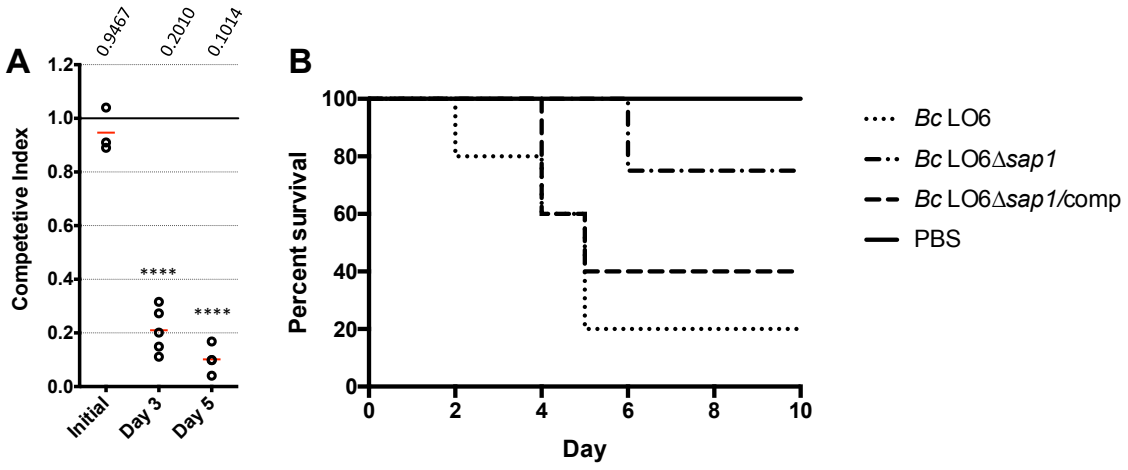

Figure 6. Comparative fitness and survival curve of mice groups. (A) CI from mouse lungs at 3 and 5 dpi, as well as the initial *in vitro* inoculum, of ~7×10^7 CFU/mouse at a 1:1 mutant to complement ratio inoculated via intratracheal intubation. Average CIs are listed at the top. **** $p<0.0001$ as determined by *t*-test. (B) Survival curve of LO6 wildtype (n=4), Δ*sap1* mutant (n=5), the complement (n=5) and PBS control (n=4).

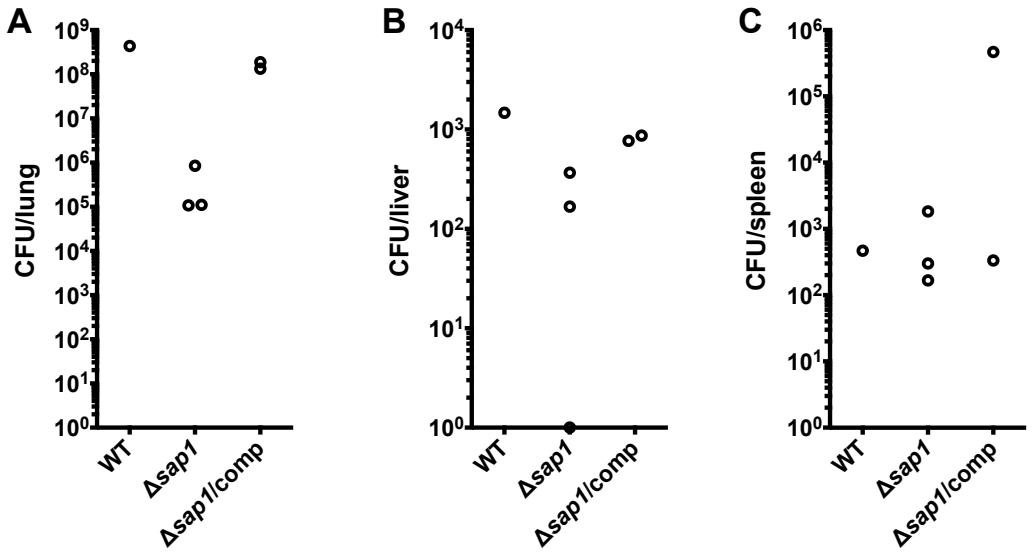

Figure 7. Bacterial loads of organs in surviving mice. Mice to survive to the end of the study had their (A) lungs, (B) livers, and (C) spleens harvested to determine CFUs.

References Cited

1. **Mahenthiralingam E**, **Baldwin A**, **Dowson CG**. 2008. Burkholderia cepacia complex bacteria: Opportunistic pathogens with important natural biology. J Appl Microbiol **104**:1539–1551.
2. **Ussery DW**, **Kiil K**, **Lagesen K**, **Sicheritz-Pont??n T**, **Bohlin J**, **Wassenaar TM**. 2009. The genus Burkholderia: Analysis of 56 genomic sequences. Genome Dyn.
3. **Loutet SA**, **Valvano MA**. 2010. A decade of Burkholderia cenocepacia virulence determinant research. Infect Immun **78**:4088–4100.
4. **Martina P**, **Feliziani S**, **Juan C**, **Bettiol M**, **Gatti B**, **Yantorno O**, **Smania AM**, **Oliver A**, **Bosch A**. 2014. Hypermutation in Burkholderia cepacia complex is mediated by DNA mismatch repair inactivation and is highly prevalent in cystic fibrosis chronic respiratory infection. Int J Med Microbiol **304**:1182–1191.
5. **Lessie TG**, **Hendrickson W**, **Manning BD**, **Devereux R**. 1996. Genomic complexity and plasticity of Burkholderia cepacia. FEMS Microbiol Lett.
6. **Oliver A**, **Mena A**. 2010. Bacterial hypermutation in cystic fibrosis, not only for antibiotic resistance. Clin Microbiol Infect **16**:798–808.
7. **Drevinek P**, **Baldwin A**, **Lindenburg L**, **Joshi LT**, **Marchbank A**, **Vosahlikova S**, **Dowson CG**, **Mahenthiralingam E**. 2010. Oxidative stress of burkholderia cenocepacia induces insertion sequence-mediated genomic rearrangements that interfere with macrorestriction-based genotyping. J Clin Microbiol **48**:34–40.
8. **Burkholder WH**. 1950. Sour skin, a bacterial rot of {Onion} bulbs. Phytopathology **40**:115--117 .
9. **Yabuuchi E**, **Kosako Y**, **Oyaizu H**, **Yano I**, **Hotta H**, **Hashimoto Y**, **Ezaki T**, **Arakawa M**. 1992. Proposal of *Burkholderia* gen. nov. and Transfer of Seven Species of the Genus *Pseudomonas* Homology Group II to the New Genus, with the Type Species *Burkholderia cepacia* (Palleroni and Holmes 1981) comb. nov. Microbiol Immunol **36**:1251–1275.
10. **Vandamme P**, **Holmes B**, **Vancanneyt M**, **Coenye T**, **Hoste B**, **Coopman R**, **Revets H**, **Lauwers S**, **Gillis M**, **Kersters K**, **Govan JRW**. 1997. Occurrence of Multiple Genomovars of Burkholderia cepacia in Cystic Fibrosis Patients and Proposal of Burkholderia multivorans sp. nov. Int J Syst Bacteriol **47**:1188–1200.
11. **Mahenthiralingam E**, **Urban TA**, **Goldberg JB**. 2005. The multifarious, multireplicon Burkholderia cepacia complex. Nat Rev Microbiol **3**:144–156.
12. **Isles A**, **Maclusky I**, **Corey M**, **Gold R**, **Prober C**, **Fleming P**, **Levison H**. 1984. Pseudomonas cepacia infection in cystic fibrosis: An emerging problem. J Pediatr **104**:206–210.
13. **Goldmann DA**, **Klinger JD**. 1986. Pseudomonas cepacia: Biology, mechanisms of virulence, epidemiology. J Pediatr **108**:806–812.
14. **LiPuma JJ**, **Dasen SE**, **Stull TL**, **Nielson DW**, **Stern RC**. 1990. Person-to-person transmission of *Pseudomonas cepacia* between patients with cystic fibrosis. Lancet **336**:1094–1096.
15. **Govan JRW**, **Doherty CJ**, **Nelson JW**, **Brown PH**, **Greening AP**, **Maddison J**, **Dodd M**, **Webb AK**. 1993. Evidence for transmission of Pseudomonas cepacia by social contact

in cystic fibrosis. Lancet **342**:15–19.
16. **Lewin C**, **Doherty C**, **Govan J**. 1993. In vitro activities of meropenem, PD 127391, PD 131628, ceftazidime, chloramphenicol, co-trimoxazole, and ciprofloxacin against Pseudomonas cepacia. Antimicrob Agents Chemother.
17. **Geftic SG**, **Heymann H**, **Adair FW**. 1979. Fourteen year survival of Pseudomonas cepacia in a salts solution preserved with benzalkonium chloride. Appl Environ Microbiol **37**:505–510.
18. **Gibson RL**, **Burns JL**, **Ramsey BW**. 2003. Pathophysiology and Management of Pulmonary Infections in Cystic Fibrosis. Am J Respir Crit Care Med **168**:918–951.
19. **Castellani C**, **Cuppens H**, **Macek M**, **Cassiman JJ**, **Kerem E**, **Durie P**, **Tullis E**, **Assael BM**, **Bombieri C**, **Brown A**, **Casals T**, **Claustres M**, **Cutting GR**, **Dequeker E**, **Dodge J**, **Doull I**, **Farrell P**, **Ferec C**, **Girodon E**, **Johannesson M**, **Kerem B**, **Knowles M**, **Munck A**, **Pignatti PF**, **Radojkovic D**, **Rizzotti P**, **Schwarz M**, **Stuhrmann M**, **Tzetis M**, **Zielenski J**, **Elborn JS**. 2008. Consensus on the use and interpretation of cystic fibrosis mutation analysis in clinical practice. J Cyst Fibros **7**:179–196.
20. **Elborn JS**. 2016. Cystic fibrosis. Lancet **388**:2519–2531.
21. **Rowe SM**, **Miller S**, **Sorscher EJ**. 2005. Cystic Fibrosis. N Engl J Med **352**:1992–2001.
22. **Farrell PM**. 2008. The prevalence of cystic fibrosis in the European Union. J Cyst Fibros **7**:450–453.
23. **Stressmann FA**, **Rogers GB**, **Klem ER**, **Lilley AK**, **Donaldson SH**, **Daniels TW**, **Carroll MP**, **Patel N**, **Forbes B**, **Boucher RC**, **Wolfgang MC**, **Bruce KD**. 2011. Analysis of the bacterial communities present in lungs of patients with cystic fibrosis from American and British centers. J Clin Microbiol **49**:281–91.
24. **LiPuma JJ**. 2010. The Changing Microbial Epidemiology in Cystic Fibrosis. Clin Microbiol Rev **23**:299–323.
25. **Magalhães AP**, **Lopes SP**, **Pereira MO**. 2017. Insights into Cystic Fibrosis Polymicrobial Consortia: The Role of Species Interactions in Biofilm Development, Phenotype, and Response to In-Use Antibiotics. Front Microbiol **7**:2146.
26. **Collawn JF**, **Matalon S**. 2014. CFTR and lung homeostasis. AJP Lung Cell Mol Physiol **307**:L917–L923.
27. **Parkins MD**, **Floto RA**. 2015. Emerging bacterial pathogens and changing concepts of bacterial pathogenesis in cystic fibrosis. J Cyst Fibros **14**:293–304.
28. **De Soyza A**, **Meachery G**, **Hester KLM**, **Nicholson A**, **Parry G**, **Tocewicz K**, **Pillay T**, **Clark S**, **Lordan JL**, **Schueler S**, **Fisher AJ**, **Dark JH**, **Gould FK**, **Corris P a**. 2010. Lung transplantation for patients with cystic fibrosis and Burkholderia cepacia complex infection: a single-center experience. J Heart Lung Transplant **29**:1395–1404.
29. **Stephenson AL**, **Sykes J**, **Berthiaume Y**, **Singer LG**, **Aaron SD**, **Whitmore GA**, **Stanojevic S**. 2015. Clinical and demographic factors associated with post–lung transplantation survival in individuals with cystic fibrosis. J Hear Lung Transplant **34**:1139–1145.
30. **Tomich M**. 2002. Role of Flagella in Host Cell Invasion by Burkholderia cepacia. Infect Immun **70**:1799–1806.
31. **McClean S**, **Callaghan M**. 2009. Burkholderia cepacia complex: Epithelial cell-pathogen confrontations and potential for therapeutic intervention. J Med Microbiol.
32. **Saldias MS**, **Valvano MA**. 2009. Interactions of Burkholderia cenocepacia and other

Burkholderia cepacia complex bacteria with epithelial and phagocytic cells. Microbiology **155**:2809–2817.
33. **Kalferstova L**, **Kolar M**, **Fila L**, **Vavrova J**, **Drevinek P**. 2015. Gene Expression Profiling of Burkholderia cenocepacia at the Time of Cepacia Syndrome: Loss of Motility as a Marker of Poor Prognosis? J Clin Microbiol **53**:1515–1522.
34. **Cunha M V.**, **Leitão JH**, **Mahenthiralingam E**, **Vandamme P**, **Lito L**, **Barreto C**, **Salgado MJ**, **Sá-Correia I**. 2003. Molecular analysis of Burkholderia cepacia complex isolates from a Portuguese cystic fibrosis center: A 7-year study. J Clin Microbiol **41**:4113–4120.
35. **Valvano MA**. 2015. Intracellular survival of Burkholderia cepacia complex in phagocytic cells 1. Can J Microbiol **61**:607–615.
36. **Sajjan SU**, **Carmody L a**, **Gonzalez CF**, **LiPuma JJ**. 2008. A Type IV Secretion System Contributes to Intracellular Survival and Replication of Burkholderia cenocepacia. Infect Immun **76**:5447–5455.
37. **Pradenas G**, **Ross B**, **Torres A**. 2016. Burkholderia cepacia Complex Vaccines: Where Do We Go from here? Vaccines **4**:10.
38. **Uehlinger S**, **Schwager S**, **Bernier SP**, **Riedel K**, **Nguyen DT**, **Sokol PA**, **Eberl L**. 2009. Identification of specific and universal virulence factors in Burkholderia cenocepacia strains by using multiple infection hosts. Infect Immun **77**:4102–4110.
39. **Leitão JH**, **Sousa SA**, **Ferreira AS**, **Ramos CG**, **Silva IN**, **Moreira LM**. 2010. Pathogenicity, virulence factors, and strategies to fight against Burkholderia cepacia complex pathogens and related species. Appl Microbiol Biotechnol **87**:31–40.
40. **Sousa SA**, **Feliciano JR**, **Pita T**, **Guerreiro SI**, **Leitão JH**. 2017. Burkholderia cepacia Complex Regulation of Virulence Gene Expression: A Review. Genes (Basel) **8**.
41. **Mil-Homens D**, **Pinto SN**, **Matos RG**, **Arraiano C**, **Fialho AM**. 2017. Burkholderia cenocepacia K56-2 trimeric autotransporter adhesin BcaA binds TNFR1 and contributes to induce airway inflammation. Cell Microbiol **19**:e12677.
42. **McClean S**, **Healy ME**, **Collins C**, **Carberry S**, **O'Shaughnessy L**, **Dennehy R**, **Adams Á**, **Kennelly H**, **Corbett JM**, **Carty F**, **Cahill LA**, **Callaghan M**, **English K**, **Mahon BP**, **Doyle S**, **Shinoy M**. 2016. Linocin and OmpW Are Involved in Attachment of the Cystic Fibrosis-Associated Pathogen Burkholderia cepacia Complex to Lung Epithelial Cells and Protect Mice against Infection. Infect Immun **84**:1424–1437.
43. **Makidon PE**, **Knowlton J**, **Groom J V.**, **Blanco LP**, **LiPuma JJ**, **Bielinska AU**, **Baker JR**. 2010. Induction of immune response to the 17?kDa OMPA Burkholderia cenocepacia polypeptide and protection against pulmonary infection in mice after nasal vaccination with an OMP nanoemulsion-based vaccine. Med Microbiol Immunol **199**:81–92.
44. **Dennehy R**, **Romano M**, **Ruggiero A**, **Mohamed YF**, **Dignam SL**, **Mujica Troncoso C**, **Callaghan M**, **Valvano MA**, **Berisio R**, **McClean S**. 2016. The Burkholderia cenocepacia peptidoglycan-associated lipoprotein is involved in epithelial cell attachment and elicitation of inflammation. Cell Microbiol 1–16.
45. **Sajjan US**, **Sylvester FA**, **Forstner JF**. 2000. Cable-Piliated Burkholderia cepacia Binds to Cytokeratin 13 of Epithelial Cells. Infect Immun **68**:1787–1795.
46. **Sajjan US**, **Forstner JF**. 1993. Role of a 22-kilodalton pilin protein in binding of Pseudomonas cepacia to buccal epithelial cells. Infect Immun **61**:3157–63.
47. **Sass A**, **Marchbank A**, **Tullis E**, **LiPuma JJ**, **Mahenthiralingam E**. 2011. Spontaneous

and evolutionary changes in the antibiotic resistance of Burkholderia cenocepacia observed by global gene expression analysis. BMC Genomics **12**:373.
48. **Urban TA**, **Griffith A**, **Torok AM**, **Smolkin ME**, **Burns JL**, **Goldberg JB**. 2004. Contribution of Burkholderia cenocepacia Flagella to Infectivity and Inflammation. Infect Immun **72**:5126–5134.
49. **Leo JC**, **Grin I**, **Linke D**. 2012. Type V secretion: mechanism(s) of autotransport through the bacterial outer membrane. Philos Trans R Soc Lond B Biol Sci **367**:1088–101.
50. **Mil-Homens D**, **Leç MI**, **Fernandes F**, **Pinto SN**, **Fialho AM**. 2014. Characterization of BCAM0224, a multifunctional trimeric autotransporter from the human pathogen Burkholderia cenocepacia. J Bacteriol **196**:1968–1979.
51. **Cunha M V.**, **Sousa SA**, **Leitão JH**, **Moreira LM**, **Videira PA**, **Sá-Correia I**. 2004. Studies on the involvement of the exopolysaccharide produced by cystic fibrosis-associated isolates of the Burkholderia cepacia complex in biofilm formation and in persistence of respiratory infections. J Clin Microbiol **42**:3052–3058.
52. **Sousa S a**, **Ulrich M**, **Bragonzi A**, **Burke M**, **Worlitzsch D**, **Leitão JH**, **Meisner C**, **Eberl L**, **Sá-Correia I**, **Döring G**. 2007. Virulence of Burkholderia cepacia complex strains in gp91phox-/- mice. Cell Microbiol **9**:2817–25.
53. **Bylund J**, **Burgess LA**, **Cescutti P**, **Ernst RK**, **Speert DP**. 2006. Exopolysaccharides from Burkholderia cenocepacia inhibit neutrophil chemotaxis and scavenge reactive oxygen species. J Biol Chem **281**:2526–2532.
54. **Estrela AB**, **Heck MG**, **Abraham WR**. 2009. Novel approaches to control biofilm infections. Curr Med Chem **16**:1512–1530.
55. **Caraher E**, **Reynolds G**, **Murphy P**, **McClean S**, **Callaghan M**. 2007. Comparison of antibiotic susceptibility of Burkholderia cepacia complex organisms when grown planktonically or as biofilm in vitro. Eur J Clin Microbiol Infect Dis **26**:213–216.
56. **Conway BD**, **Venu V**, **Speert DP**. 2002. Biofilm Formation and Acyl Homoserine Lactone Production in the Burkholderia cepacia Complex. J Bacteriol **184**:5678–5685.
57. **Bragonzi A**, **Farulla I**, **Paroni M**, **Twomey KB**, **Pirone L**, **Lorè NI**, **Bianconi I**, **Dalmastri C**, **Ryan RP**, **Bevivino A**. 2012. Modelling Co-Infection of the Cystic Fibrosis Lung by Pseudomonas aeruginosa and Burkholderia cenocepacia Reveals Influences on Biofilm Formation and Host Response. PLoS One **7**:e52330.
58. **Steidle A**, **Eberl L**, **Wu H**, **Geisenberger O**, **Molin S**, **Huber B**, **Riedel K**, **Hentzer M**, **Høiby N**, **Givskov M**. 2001. N-Acylhomoserine-lactone-mediated communication between Pseudomonas aeruginosa and Burkholderia cepacia in mixed biofilms. Microbiology **147**:3249–3262.
59. **Schwab U**, **Leigh M**, **Ribeiro C**, **Yankaskas J**, **Burns K**, **Gilligan P**, **Sokol P**, **Boucher R**. 2002. Patterns of epithelial cell invasion by different species of the Burkholderia cepacia complex in well-differentiated human airway epithelia. Infect Immun **70**:4547–4555.
60. **Winsor GL**, **Khaira B**, **Van Rossum T**, **Lo R**, **Whiteside MD**, **Brinkman FSL**. 2008. The Burkholderia Genome Database: facilitating flexible queries and comparative analyses. Bioinformatics **24**:2803–2804.
61. **Kang Y**, **Norris MH**, **Barrett AR**, **Wilcox B a**, **Hoang TT**. 2009. Engineering of tellurite-resistant genetic tools for single-copy chromosomal analysis of Burkholderia spp. and characterization of the Burkholderia thailandensis betBA operon. Appl Environ

Microbiol **75**:4015–27.
62. **Norris MH**, **Kang Y**, **Lu D**, **Wilcox BA**, **Hoang TT**. 2009. Glyphosate resistance as a novel select-agent-compliant, non-antibiotic-selectable marker in chromosomal mutagenesis of the essential genes asd and dapB of Burkholderia pseudomallei. Appl Environ Microbiol **75**:6062–6075.
63. **Sambrook J**, **W Russell D**. 2012. Molecular Cloning: A Laboratory ManualCold Spring Harbor Laboratory Press, Cold Spring Harbor, NY.
64. **Barrett AR**, **Kang Y**, **Inamasu KS**, **Son MS**, **Vukovich JM**, **Hoang TT**. 2008. Genetic tools for allelic replacement in Burkholderia species. Appl Env Microbiol **74**:4498–4508.
65. **Kang Y**, **Norris MH**, **Wilcox BA**, **Tuanyok A**, **Keim PS**, **Hoang TT**. 2011. Knockout and pullout recombineering for naturally transformable Burkholderia thailandensis and Burkholderia pseudomallei. Nat Protoc **6**:1085–104.
66. **Norris MH**, **Kang Y**, **Wilcox B**, **Hoang TT**. 2010. Stable, site-specific fluorescent tagging constructs optimized for burkholderia species. Appl Environ Microbiol **76**:7635–7640.
67. **O'Toole GA**. 2011. Microtiter Dish Biofilm Formation Assay. J Vis Exp e2437–e2437.
68. **Merritt JH**, **Kadouri DE**, **O'Toole GA**. 2005. Growing and Analyzing Static BiofilmsCurrent Protocols in Microbiology. John Wiley & Sons, Inc., Hoboken, NJ, USA.
69. **Tram G**, **Korolik V**, **Day CJ**. 2013. MBDS Solvent: An Improved Method for Assessment of Biofilms. Adv Microbiol **3**:200–204.
70. **Brenner S**. THE GENETICS OF CAENORHABDZTZS ELEGANS.
71. **Tan M-W**, **Rahme LG**, **Sternberg JA**, **Tompkins RG**, **Ausubel FM**. 1999. Pseudomonas aeruginosa killing of Caenorhabditis elegans used to identify P. aeruginosa virulence factors **96**:2408–2413.
72. **Castonguay-Vanier J**, **Vial L**, **Tremblay J**, **Déziel E**. 2010. Drosophila melanogaster as a Model Host for the Burkholderia cepacia Complex. PLoS One **5**:e11467.
73. **Brickman TJ**, **Vanderpool CK**, **Armstrong SK**. 2006. Heme transport contributes to in vivo fitness of Bordetella pertussis during primary infection in mice. Infect Immun **74**:1741–4.
74. **Sousa SA**, **Ramos CG**, **Leitão JH**. 2011. Burkholderia cepacia Complex: Emerging Multihost Pathogens Equipped with a Wide Range of Virulence Factors and Determinants. Int J Microbiol **2011**:1–9.
75. **Paganin P**, **Fiscarelli EV**, **Tuccio V**, **Chiancianesi M**, **Bacci G**, **Morelli P**, **Dolce D**, **Dalmastri C**, **De Alessandri A**, **Lucidi V**, **Taccetti G**, **Mengoni A**, **Bevivino A**. 2015. Changes in Cystic Fibrosis Airway Microbial Community Associated with a Severe Decline in Lung Function. PLoS One **10**:e0124348.
76. **Lamothe J**, **Huynh KK**, **Grinstein S**, **Valvano MA**. 2007. Intracellular survival of Burkholderia cenocepacia in macrophages is associated with a delay in the maturation of bacteria-containing vacuoles. Cell Microbiol **9**:40–53.
77. **Bernier SP**, **Sokol PA**. 2005. Use of Suppression-Subtractive Hybridization To Identify Genes in the Burkholderia cepacia Complex That Are Unique to Burkholderia cenocepacia. J Bacteriol **187**:5278–5291.
78. **Ronning CM**, **Losada L**, **Brinkac L**, **Inman J**, **Ulrich RL**, **Schell M**, **Nierman WC**, **Deshazer D**. 2010. Genetic and phenotypic diversity in Burkholderia: contributions by prophage and phage-like elements. BMC Microbiol **10**:202.

79. **Biddick R**, **Spilker T**, **Martin A**, **LiPuma JJ**. 2003. Evidence of transmission of Burkholderia cepacia , Burkholderia multivorans and Burkholderia dolosa among persons with cystic fibrosis. FEMS Microbiol Lett **228**:57–62.
80. **Vermis K**, **Coenye T**, **LiPuma JJ**, **Mahenthiralingam E**, **Nelis HJ**, **Vandamme P**. 2004. Proposal to accommodate Burkholderia cepacia genomovar VI as Burkholderia dolosa sp. nov. Int J Syst Evol Microbiol **54**:689–691.
81. **Vermis K**, **Coenye T**, **Mahenthiralingam E**, **Nelis HJ**, **Vandamme P**. 2002. Evaluation of species-specific recA-based PCR tests for genomovar level identification within the Burkholderia cepacia complex. J Med Microbiol **51**:937–940.
82. **Govan JR**, **Deretic V**. 1996. Microbial pathogenesis in cystic fibrosis: mucoid Pseudomonas aeruginosa and Burkholderia cepacia. Microbiol Rev **60**:539–74.
83. **Köthe M**, **Antl M**, **Huber B**, **Stoecker K**, **Ebrecht D**, **Steinmetz I**, **Eberl L**. 2003. Killing of *Caenorhabditis elegans* by *Burkholderia cepacia* is controlled by the cep quorum-sensing system. Cell Microbiol **5**:343–351.
84. **Begun J**, **Gaiani JM**, **Rohde H**, **Mack D**, **Calderwood SB**, **Ausubel FM**, **Sifri CD**. 2007. Staphylococcal biofilm exopolysaccharide protects against Caenorhabditis elegans immune defenses. PLoS Pathog **3**:526–540.
85. **Sibley CD**, **Duan K**, **Fischer C**, **Parkins MD**, **Storey DG**, **Rabin HR**, **Surette MG**. 2008. Discerning the Complexity of Community Interactions Using a Drosophila Model of Polymicrobial Infections. PLoS Pathog **4**:e1000184.
86. **Mulcahy H**, **Sibley CD**, **Surette MG**, **Lewenza S**. 2011. Drosophila melanogaster as an Animal Model for the Study of Pseudomonas aeruginosa Biofilm Infections In Vivo. PLoS Pathog **7**:e1002299.
87. **Lee AH-Y**, **Flibotte S**, **Sinha S**, **Paiero A**, **Ehrlich RL**, **Balashov S**, **Ehrlich GD**, **Zlosnik JEA**, **Mell JC**, **Nislow C**. 2017. Phenotypic diversity and genotypic flexibility of Burkholderia cenocepacia during long-term chronic infection of cystic fibrosis lungs. Genome Res **27**:650–662.
88. **Schwab U**, **Abdullah LH**, **Perlmutt OS**, **Albert D**, **Davis CW**, **Arnold RR**, **Yankaskas JR**, **Gilligan P**, **Neubauer H**, **Randell SH**, **Boucher RC**. 2014. Localization of Burkholderia cepacia Complex Bacteria in Cystic Fibrosis Lungs and Interactions with Pseudomonas aeruginosa in Hypoxic Mucus. Infect Immun **82**:4729–4745.
89. **Cullen L**, **Mcclean S**. 2015. Bacterial Adaptation during Chronic Respiratory Infections. Pathogens **4**:66–89.
90. **Vandamme P**, **Holmes B**, **Coenye T**, **Goris J**, **Mahenthiralingam E**, **LiPuma JJ**, **Govan JRW**. 2003. Burkholderia cenocepacia sp. nov.--a new twist to an old story. Res Microbiol **154**:91–6.
91. **Vandamme P**, **Mahenthiralingam E**, **Holmes B**, **Coenye T**, **Hoste B**, **De Vos P**, **Henry D**, **Speert DP**. 2000. Identification and population structure of Burkholderia stabilis sp. nov. (formerly Burkholderia cepacia genomovar IV). J Clin Microbiol **38**:1042–1047.
92. **Coenye T**, **Mahenthiralingam E**, **Henry D**, **LiPuma JJ**, **Laevens S**, **Gillis M**, **Speert DP**, **Vandamme P**. 2001. *Burkholderia ambifaria* sp. nov., a novel member of the *Burkholderia cepacia* complex including biocontrol and cystic fibrosis-related isolates. Int J Syst Evol Microbiol **51**:1481–1490.
93. **Vandamme P**, **Henry D**, **Coenye T**, **Nzula S**, **Vancanneyt M**, **LiPuma JJ**, **Speert DP**, **Govan JRW**, **Mahenthiralingam E**. 2002. Burkholderia anthina sp. nov. and

Burkholderia pyrrocinia, two additional Burkholderia cepacia complex bacteria, may confound results of new molecular diagnostic tools. FEMS Immunol Med Microbiol **33**:143–149.

94. **Vanlaera E**, **LiPuma JJ**, **Baldwin A**, **Henry D**, **Brandt E De**, **Mahenthiralingam E**, **Speert D**, **Dowson C**, **Vandamme P**. 2008. Burkholderia latens sp. nov., Burkholderia diffusa sp. nov., Burkholderia arboris sp. nov., Burkholderia seminalis sp. nov., and Burkholderia metallica sp. nov., novel species within the Burkholderia cepacia complex. Int J Syst Evol Microbiol **58**:1580–1590.
95. **Vanlaere E**, **Baldwin A**, **Gevers D**, **Henry D**, **De Brandt E**, **LiPuma JJ**, **Mahenthiralingam E**, **Speert DP**, **Dowson C**, **Vandamme P**. 2009. Taxon K, a complex within the Burkholderia cepacia complex, comprises at least two novel species, Burkholderia contaminans sp. nov. and Burkholderia lata sp. nov. Int J Syst Evol Microbiol **59**:102–111.
96. **Peeters C**, **Zlosnik JEA**, **Spilker T**, **Hird TJ**, **LiPuma JJ**, **Vandamme P**. 2013. Burkholderia pseudomultivorans sp. nov., a novel Burkholderia cepacia complex species from human respiratory samples and the rhizosphere. Syst Appl Microbiol **36**:483–489.
97. **De Smet B**, **Mayo M**, **Peeters C**, **Zlosnik JEA**, **Spilker T**, **Hird TJ**, **Li Puma JJ**, **Kidd TJ**, **Kaestli M**, **Ginther JL**, **Wagner DM**, **Keim P**, **Bell SC**, **Jacobs JA**, **Currie BJ**, **Vandamme P**. 2015. Burkholderia stagnalis sp. nov. and Burkholderia territorii sp. nov., two novel Burkholderia cepacia complex species from environmental and human sources. Int J Syst Evol Microbiol **65**:2265–2271.
98. **Figurski DH**, **Helinski DR**. 1979. Replication of an origin-containing derivative of plasmid RK2 dependent on a plasmid function provided in trans. Proc Natl Acad Sci U S A **76**:1648–52.